J. Fluid Mech. (1987), *vol.* 184, *pp.* 1–14
Printed in Great Britain

The effects of surface tension and tube inclination on a two-dimensional rising bubble

By BENOIT COUËT† AND GARY S. STRUMOLO‡
Schlumberger-Doll Research, Old Quarry Road, Ridgefield, CT 06877-4108, USA

(Received 5 September 1986 and in revised form 18 March 1987)

The effects of surface tension σ and tube inclination β on the Froude number Fr of a large bubble rising in a two-dimensional duct is considered. It is found that there exists either one (for small σ and $\beta > 0°$) or a set (for any σ and $\beta = 0°$) of Fr-values for which the bubble has a continuous derivative at the nose. By selecting either this single Fr (or the maximum of the set), we obtain solutions in excellent agreement with both theoretical predictions and experimental results.

1. Introduction

The propagation rate of long bubbles in (either two- or three-dimensional) tubes has been studied both theoretically and experimentally for the past few decades. Experiments have shown the effects of fluid properties and pipe inclination on the rise velocity of these bubbles (most notably the three-dimensional work of Zukoski 1966 and the two-dimensional studies of Maneri 1970 and Maneri & Zuber 1974). Theoretical analyses have been limited to vertical flow with zero surface tension, either by setting $\sigma = 0$ directly (Dumitrescu 1943; Davies & Taylor 1950; Birkhoff & Carter 1957; Garabedian 1957; Collins 1965; Grace & Harrison 1967; Collins *et al.* 1978; Vanden-Broeck 1984*a*; and Couët, Strumolo & Dukler 1986) or by letting $\sigma \to 0$ (Vanden-Broeck 1984*b*). The purpose of our study is to provide a theoretical basis that will both describe the influence of surface tension and tube inclination on the propagation velocity, and reconcile theory with experiments in these instances.

Consider a bubble rising with velocity U in a two-dimensional duct of width $2a$. By imposing an equal but opposite flow on the system, we can locate our coordinate axes at the bubble nose, as was done by Vanden-Broeck (1984*b*) and shown in figure 1. The angle between the negative x-axis and the tangent line at the nose of the bubble is designated γ. The following dimensionless parameters play an important role in our analysis:

$$Fr = \frac{U}{(2ga)^{\frac{1}{2}}}, \tag{1}$$

$$\alpha = \frac{2\rho U^2 a}{\sigma}, \tag{2}$$

$$\Sigma = \frac{\sigma}{\rho g a^2}, \tag{3}$$

† Present address: Schlumberger Cambridge Research, P.O. Box 153, Cambridge, CB3 0HG, UK.

‡ Present address: Dowell Schlumberger, P.O. Box 2710, Tulsa, OK 74101, USA.

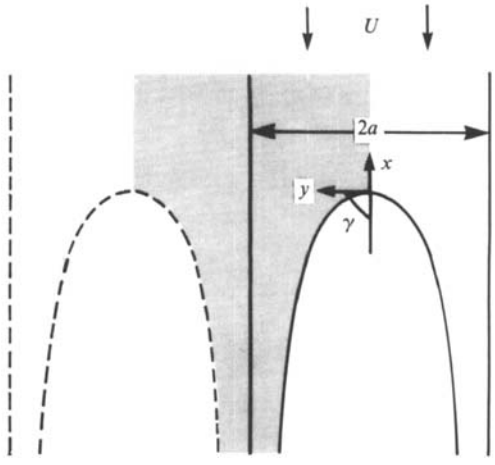

FIGURE 1. Schematic of flow field and coordinate system. Dashed lines correspond to reflection about line $y = a$. Computational domain is illustrated by the shaded region.

where g is the acceleration due to gravity, ρ is the density of the surrounding fluid, and σ the surface tension. These parameters are commonly referred to as the Froude, Weber, and inverse Eötvos numbers, respectively. Our objective is to determine how Fr varies with both Σ or β, the inclination of the duct from the vertical.

We describe our solution procedure in the next section, followed in §3 by an analysis of the vertical case ($\beta = 0°$). Section 4 presents a study of the inclined cases and some of the resulting bubble shapes are illustrated in §5.

2. Solution procedure

We ignore the effects of viscosity in the liquid and consider potential flow around the bubble (Zukoski 1966 has shown experimentally that the rise velocity of a large bubble in a tube is independent of the Reynolds number Re provided $Re > 200$). We shall determine the bubble shape by imposing the condition of constant pressure along its free surface. Bernoulli's equation shows that this requirement takes the form:

$$\tfrac{1}{2}q^2 + g(x\cos\beta + y\sin\beta) - \left(\frac{\sigma}{\rho}\right)K = B, \tag{4}$$

where q is the flow speed, K is the curvature of the free surface, and B is the Bernoulli constant. Here we have generalized to arbitrary angles of inclination the technique employed by Birkhoff & Carter (1957) and, more recently, by Vanden-Broeck (1984*a*, *b*). Details of this procedure can be found in these references. This approach leads to the following non-dimensional form for (4):

$$\pi\cot s\exp(2\tau)\frac{\mathrm{d}\tau}{\mathrm{d}s} + \frac{1}{Fr^2}(\exp(-\tau)\cos\theta\cos\beta + \exp(-\tau)\sin\theta\sin\beta) - \frac{1}{\alpha}\pi^2\cot s\frac{\mathrm{d}}{\mathrm{d}s}\left(\exp(\tau)\cot s\frac{\mathrm{d}\theta}{\mathrm{d}s}\right) = 0. \tag{5}$$

Since a rising bubble is characterized by a stagnation point at the nose and we also require symmetry about the x-axis, continuity of the bubble shape and of its slope through the nose lead us to identify the physical solutions as those for which $\gamma = \frac{1}{2}\pi$.

Using a collocation method, we select N points along the bubble surface at which (5) must be satisfied. This results in N nonlinear equations for N unknowns including the parameter γ, which we solve using Newton's method. The bubble shape can then be calculated by integrating a simple differential equation involving the complex velocity (see Vanden-Broeck 1984*b*).

3. Vertical flow ($\beta = 0°$)

Before we present the results of our numerical calculations, we should discuss what is known from experimental observations about a vertical rising large bubble. It is common experimental knowledge that a large bubble rises with a Froude number of 0.49 (0.23 in two dimensions), as shown in Zukoski (1966) and Collins (1965). This has been observed, however, only for small Σ, say, less than 0.1. As Σ increases, the Froude number decreases monotonically. This is illustrated for the case of three-dimensional flow in figure 2 (taken from Zukoski 1966, which includes data from other researchers as well as his own).

If we fix the Weber number, we can solve (5) for any value of Fr and obtain a solution for γ. The result of these calculations for three Weber numbers are shown in figure 3 (case $\alpha = 10$ is shown in Vanden-Broeck (1984*b*)). Note that each curve intersects the dashed $\gamma = \frac{1}{2}\pi$ line a countable number of times (it may even intersect a countably infinite number of times, but discrete numerical calculations obviously cannot give evidence of this). As discussed in the previous section, we identify these solutions as the only physically reasonable ones. If we take for each Weber number the maximum† Fr-value for which $\gamma = \frac{1}{2}\pi$, we obtain a relationship between Fr and Σ, illustrated in figure 4. The agreement between this two-dimensional numerical result and the three-dimensional experimental result of figure 2 is quite remarkable. While the Froude numbers are different due to the difference in dimensionality, both show that Fr is relatively constant up to $\Sigma = 0.1$, after which it drops off monotonically. Our numerical result for low Σ levels off at $Fr = 0.226$, in precise agreement with Collins's two-dimensional experimental result, where $\Sigma \approx 10^{-4}$.

At this point, it is worth taking some time to discuss previous work on the zero-surface-tension case. Dumitrescu (1943) and Davies & Taylor (1950) had to introduce the artificial constraint that the bubble nose was circular to isolate a single Fr-value; even so, the bubble did not satisfy the condition of constant pressure along its surface. Garabedian (1957) attempted a stability analysis and from his numerical results came up with a guess of $Fr = 0.24$ while Vanden-Broeck (1984*a*) estimated $Fr = 0.36$. Vanden-Broeck did not hypothesize on the discrepancy between his result and Garabedian's, but there may be a simple explanation for this.

Garabedian used only four terms in his series expansion for a functional of the complex potential f while Vanden-Broeck with a series similar to ours used many more terms to obtain his value. We ran our zero-surface-tension code for a number of different N-values. In each case, we computed the speed at the nose of the bubble. If it was zero, $\gamma = \frac{1}{2}\pi$. A plot of this normalized speed, q/U, is given in figure 5 with N ranging from 10 to 150. If γ is taken to be $\frac{1}{2}\pi$ when q/U is less than some small number, then the maximum Froude number (for which $\gamma = \frac{1}{2}\pi$) will vary with N. While the figure shows that 0.36 seems to be the limit as N approaches infinity, it also

† Why select the maximum Froude number as the one realized physically? Our reasoning follows the arguments given in Garabedian's (1957) paper, where he presented a stability argument, assuming zero surface tension, which postulated that the Froude number one would see experimentally should be the one that permits the bubble to travel at the fastest speed allowable.

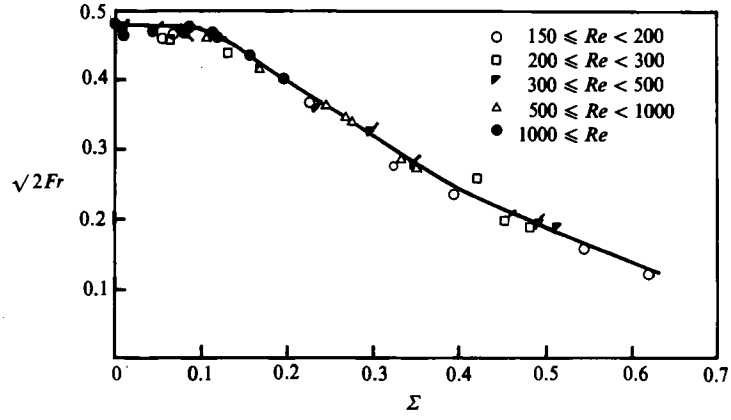

FIGURE 2. Three-dimensional experimental data on the relationship between Fr and Σ for a vertical tube (taken from Zukoski 1966).

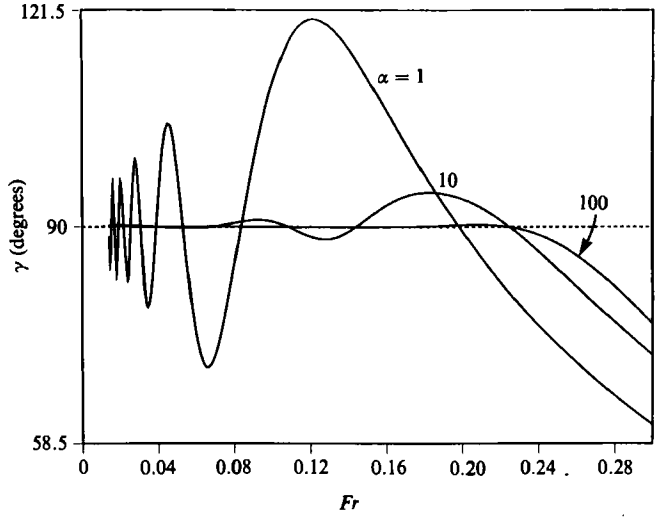

FIGURE 3. Dependence of γ on Fr for three different Weber-number cases ($\beta = 0°$).

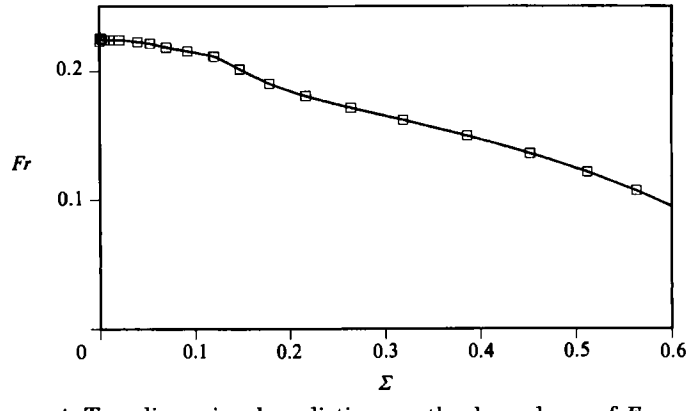

FIGURE 4. Two-dimensional predictions on the dependence of Fr on Σ ($\beta = 0°$).

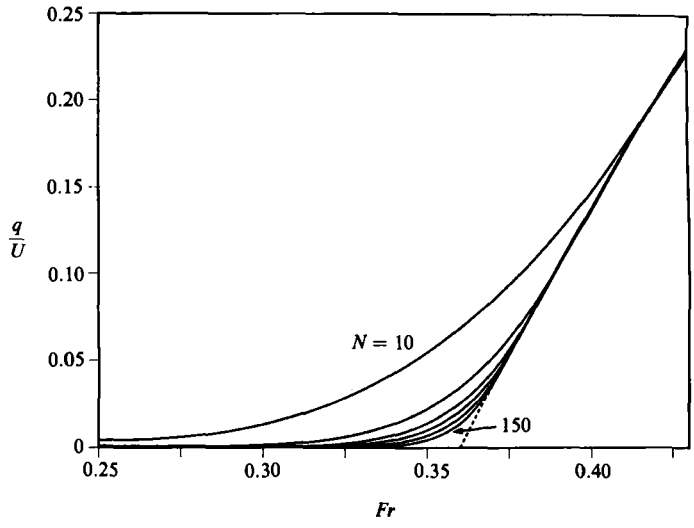

FIGURE 5. Variation of the normalized speed at the bubble nose with Fr for different values of N: 10, 30, 50, 70, 100, 150. Dashed line corresponds to limit as $N \to \infty$ ($\beta = 0°$).

shows how Garabedian could have obtained 0.24 with the small number of terms in his series. Had he used more terms, he might have obtained the same result as Vanden-Broeck, namely $Fr = 0.36$. His deriving a value near the experimentally observed one may therefore have been a result of his numerical approximation. Vanden-Broeck (1984*b*) attempted to resolve a second discrepancy, between his zero-surface-tension result of $Fr = 0.36$ and the experimental result of $Fr = 0.23$, by introducing surface-tension effects. His argument for selecting 0.23 as the critical Froude number goes as follows. For a given Weber number, there are (what may be) a countably infinite number of Froude numbers for which $\gamma = \frac{1}{2}\pi$ (see figure 3). Consider the sequence of Froude numbers corresponding to the maximum location at which $\gamma = \frac{1}{2}\pi$, the next-to-maximum location, etc. Vanden-Broeck (1984*b*) claimed that as σ approached zero ($\alpha \to \infty$), all these solutions approached a unique limiting solution with $Fr = 0.23$. This statement, however, may be misleading. As σ approaches zero, both the wavelength and the amplitude of the oscillations decrease, as is shown in figure 3. While the maximum location of a solution at which $\gamma = \frac{1}{2}\pi$ approaches 0.23, the density of solutions increases until it covers the interval $0 < Fr < 0.23$. Thus, it appears that the most he could conclude from the numerical results is that 0.23 is the least upper bound of all Froude numbers for which $\gamma = \frac{1}{2}\pi$, provided $\sigma > 0$. But by combining our numerical analysis with Garabedian's maximization argument, we not only show the dependence of Fr on Σ, but also verify the experimental results in the low-Σ range. One should keep in mind that no experimental results exist for zero surface tension.

4. Inclined flow ($\beta > 0°$)

We now incline the duct at an angle β from the vertical. Unlike the previous vertical case, when the duct is inclined there exists only one Fr-value for a sufficiently large Weber number for which $\gamma = \frac{1}{2}\pi$. This is illustrated in figure 6. (Note that when Fr approaches zero, the curves level off to $\gamma = \frac{1}{2}\pi + \beta$, which implies that at the nose the free surface is horizontal, regardless of the duct inclination.) As before, by selecting

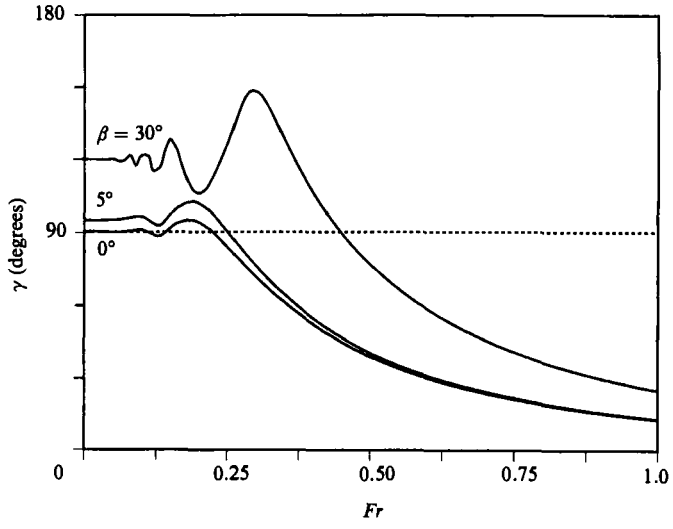

FIGURE 6. Dependence of γ on Fr for three different inclination angles ($\alpha = 10$).

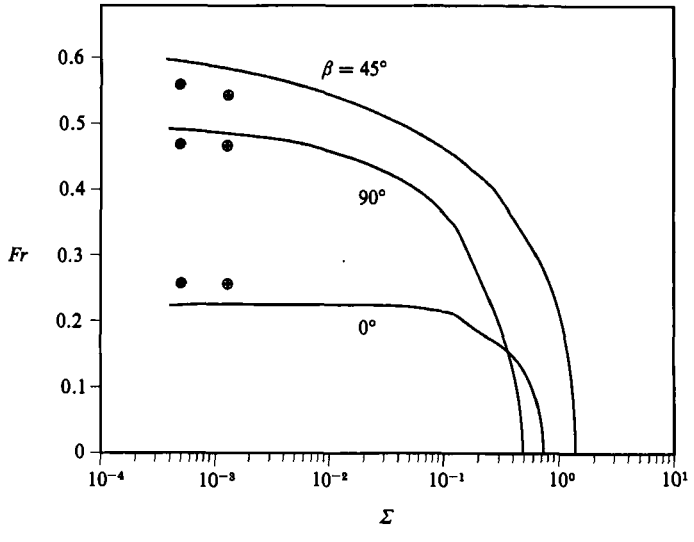

FIGURE 7. Two-dimensional predictions of the variation of Fr with Σ for three inclination angles. Dots correspond to experimental data from Maneri (1970): ⊕, water; ●, methanol.

those solutions for which $\gamma = \frac{1}{2}\pi$ we can obtain a relationship for Fr versus Σ, but now we can do it for an arbitrary inclination angle. A plot of these curves for $\beta = 0°$, 45°, and 90° is given in figure 7. Zukoski (1966) obtained three-dimensional experimental reults for the same inclination angles; these are shown in figure 8. The similarities are quite compelling.

A few points about the numerical results of figure 7 should be made. First, as Σ approaches zero for the horizontal duct ($\beta = 90°$), the Froude number approaches 0.5. This is in agreement with the theoretical analysis of Benjamin (1968). Second, by modifying the original Bernoulli equation, it was possible to determine solutions for the zero-Froude-number cases. These show that bubbles will remain fixed in

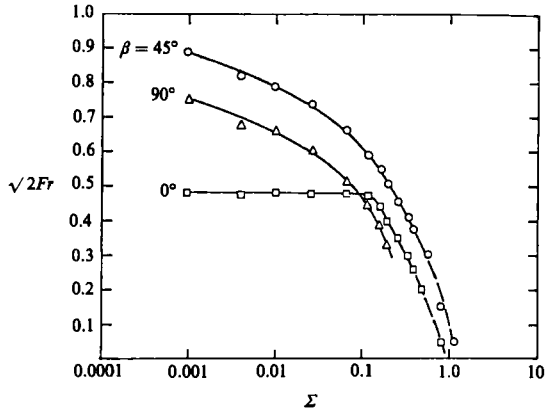

FIGURE 8. Three-dimensional experimental data on the variation of Fr with Σ for the same inclination angles as in figure 7 (taken from Zukoski 1966).

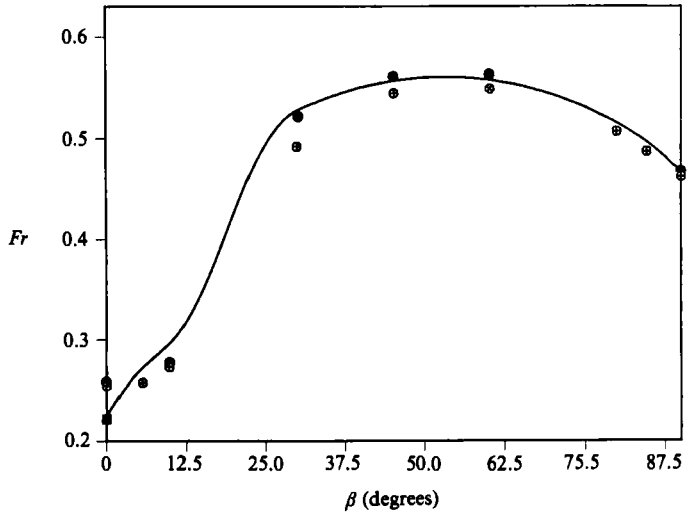

FIGURE 9. Comparison of our 'best fit' predicted curve with experimental data of Maneri (1970): ⊕, water; ●, methanol; and Collins (1965): (■).

position when the Eötvos number is of the order unity, i.e. when there is a balance between gravitational and surface tension forces.

We can also plot the dependence of Fr on inclination angle. Figure 9 compares our numerical predictions to the 'two-dimensional' experimental data of Maneri (1970) and Collins (1965) over the full range of inclination.† The agreement is quite good. Our numerical curve has a range of Σ-values approximately ten times higher than the experimental ones. This may be attributed to three-dimensional effects present in the 'two-dimensional' experiment: Collins (1965) pointed out that surface-tension effects between the bubble and the plates making up the duct can have an effect on the rise velocity.

† 'Two-dimensional' bubbles were created by injecting air into the base of a narrow rectangular duct formed by two flat plates separated by a small gap. The ratio of duct width to gap separation was either 12 or 15, providing an approximation to the two-dimensional case.

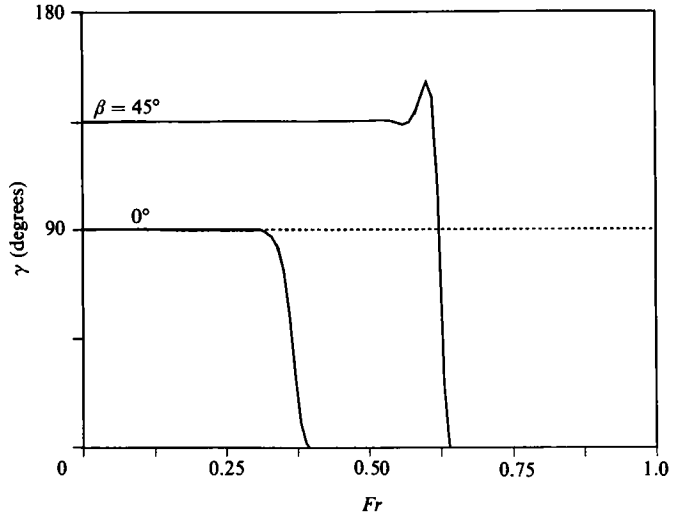

FIGURE 10. Dependence of γ on Fr in the inertial limit case ($\Sigma = 0$).

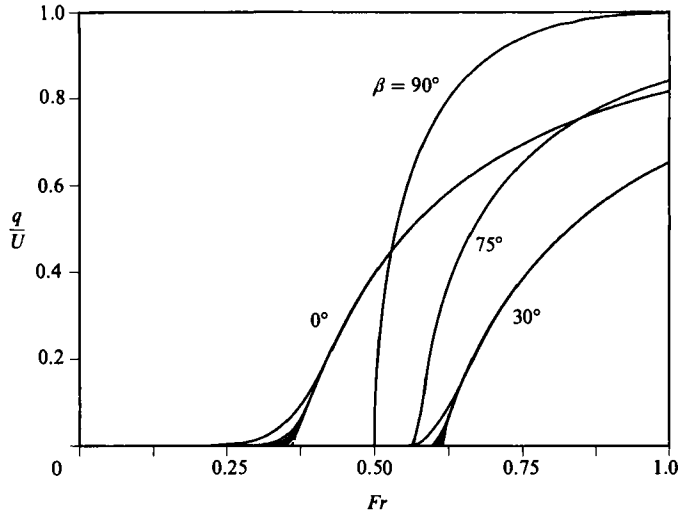

FIGURE 11. Variation of the normalized speed at the bubble nose with Fr at different inclination angles.

The limiting case of zero surface tension can also be illustrated. Figure 10 shows the relationship of γ to Fr for $\beta = 0°$ and 45°. $N = 100$ in these calculations. Figure 5 showed the normalized velocity at the nose for vertical flow. Similarly, we can also calculate these speeds for the case of inclined ducts; the results are given in figure 11 (N varies from 10 to 150). The curves become steeper as β approaches 90° with all of them obviously bounded by unity in the limit of large Froude number.

We also made numerous checks on the accuracy of our solution procedure. We found that the number of terms used in the series approximation does not play a significant role in determining the Froude number, provided it is larger than, say, 30. Taking the values at $N = 200$ as 'exact', we plot in figure 12 the per cent error as a function of N for two angles, $\beta = 45°$ and $\beta = 90°$, and for $\Sigma = 0$ and $\Sigma = 0.001$. For $N > 30$ the curves are approximately straight, implying an exponential decay with N.

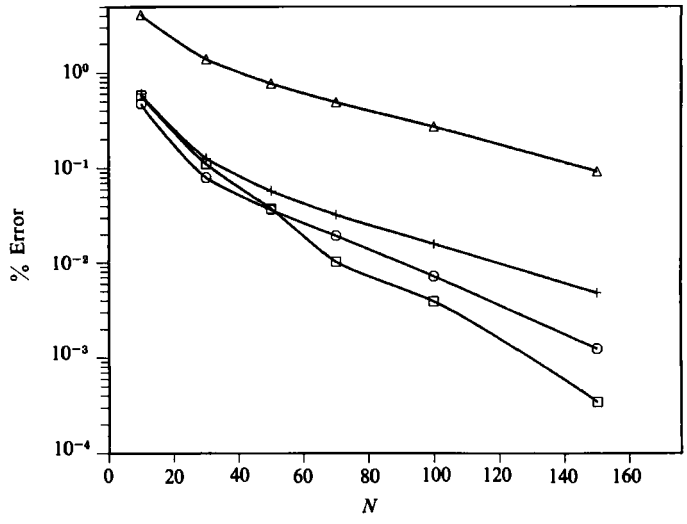

FIGURE 12. Variation of per cent error with N for the case $\Sigma = 0$: △, $\beta = 45°$; +, $\beta = 90°$; and $\Sigma = 0.001$: ○, $\beta = 90°$; □, $\beta = 45°$.

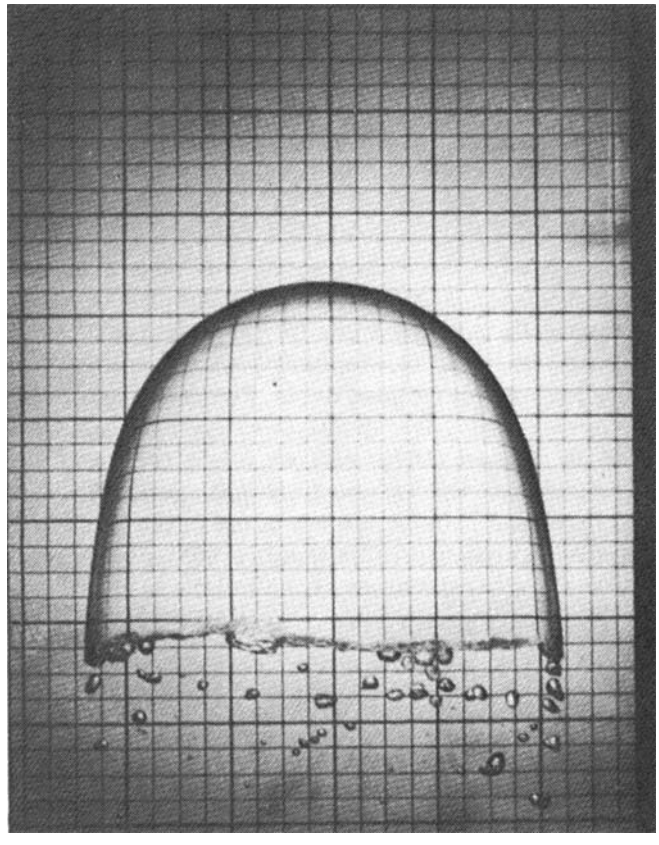

FIGURE 13. Two-dimensional experimental bubble rising in vertical duct (from Maneri 1970).

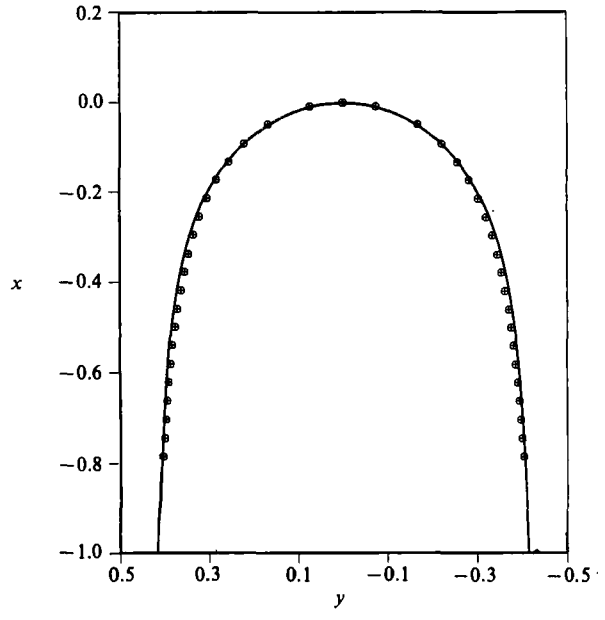

FIGURE 14. Comparison between Maneri's (1970) digitized experimental bubble: ⊕, water; and our numerically calculated one: ——.

5. Bubble shapes

In §2, we stated that the bubble shapes could be computed by integrating a simple differential equation involving the complex velocity. While our predicted Froude numbers appear to be in good agreement with experiments, do the predicted shapes also agree with those obtained experimentally? Let us begin with the vertical case. Figure 13 is a photograph of a 'two-dimensional' bubble from Maneri (1970). In his work he gave the digitized shapes for this and other bubbles. Comparing his digitized bubble with our numerically generated one for the case $\beta = 0°$, we get an excellent agreement as illustrated in figure 14. Similarly, we can compare his experimental bubbles to our numerical ones for inclined ducts. Figures 15 and 16 consider the cases of $\beta = 30°$ and $60°$, respectively. We choose the experimental Froude numbers for each angle provided by Maneri (1970) and we select the bubble shape for which $\gamma = \frac{1}{2}\pi$. As in the vertical case, the agreement is quite good. We have already noted that for $\beta = 90°$ the predicted Froude number of 0.5 in the zero-surface-tension case agrees with the theoretical prediction of Benjamin (1968). Figure 17 shows the bubble for $\beta = 90°$. Note that the final thickness of the bubble is half the duct height, also in agreement with Benjamin's predictions.

6. Conclusion

We have considered a numerical model of a large bubble rising in a two-dimensional duct. The effects of surface tension and tube inclination on both the Froude number and the bubble shape are in excellent agreement with both theoretical predictions and experimental observations.

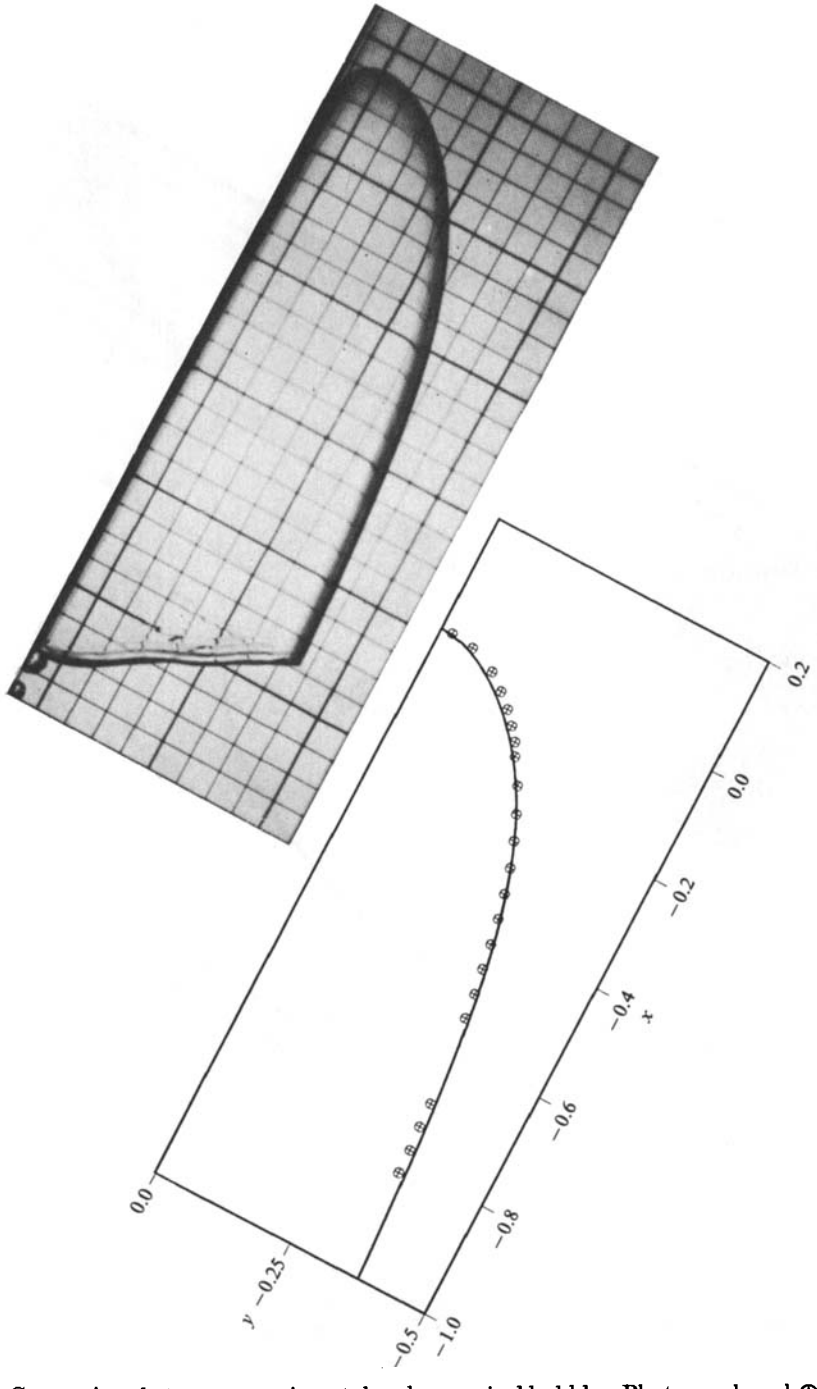

FIGURE 15. Comparison between experimental and numerical bubbles. Photograph and ⊕ are from Maneri (1970) while the solid line is our predicted bubble shape. Inclination angle $\beta = 30°$.

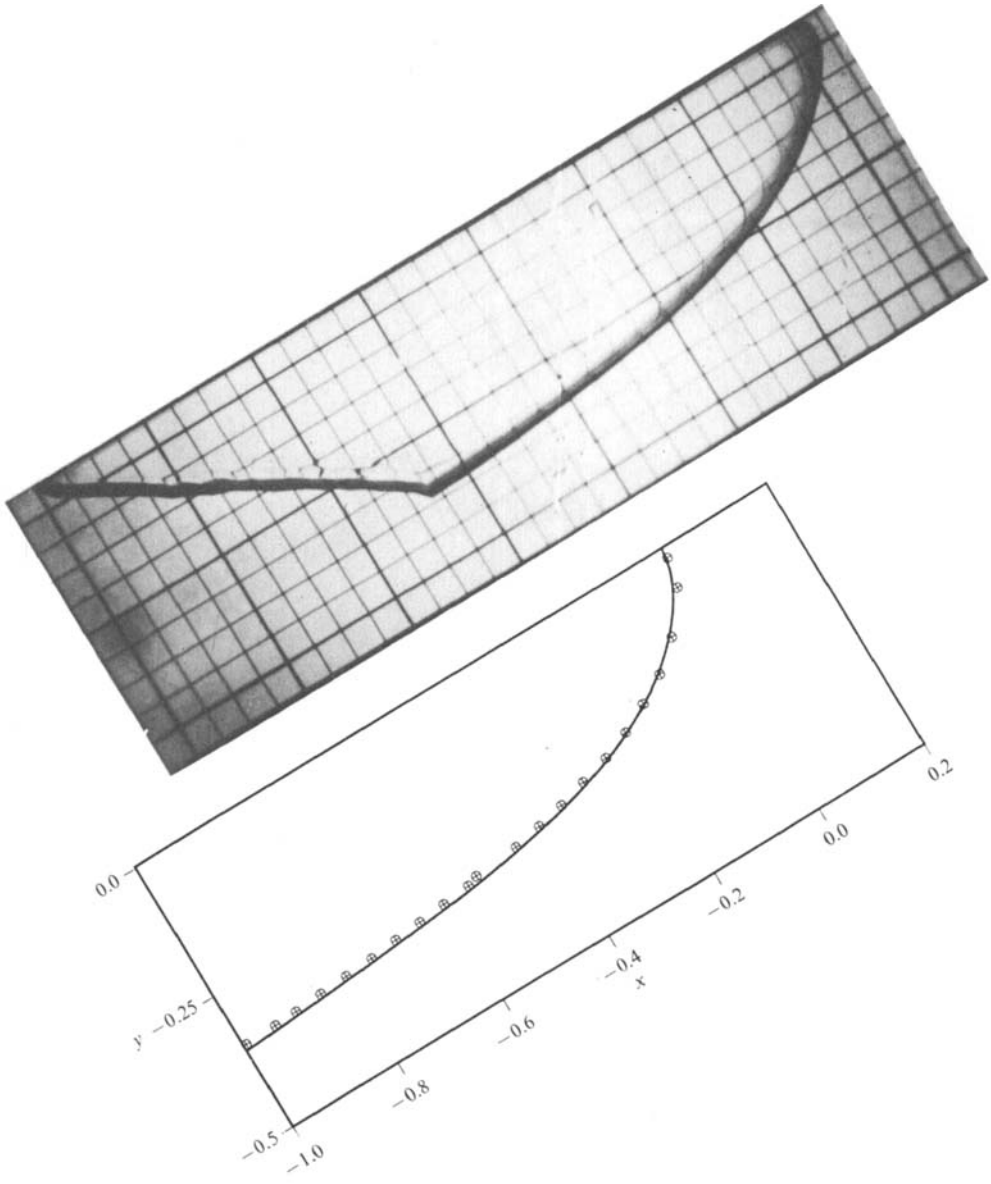

FIGURE 16. Comparison between experimental and numerical bubbles. Photograph and ⊕ are from Maneri (1970) while the solid line is our predicted bubble shape. Inclination angle $\beta = 60°$.

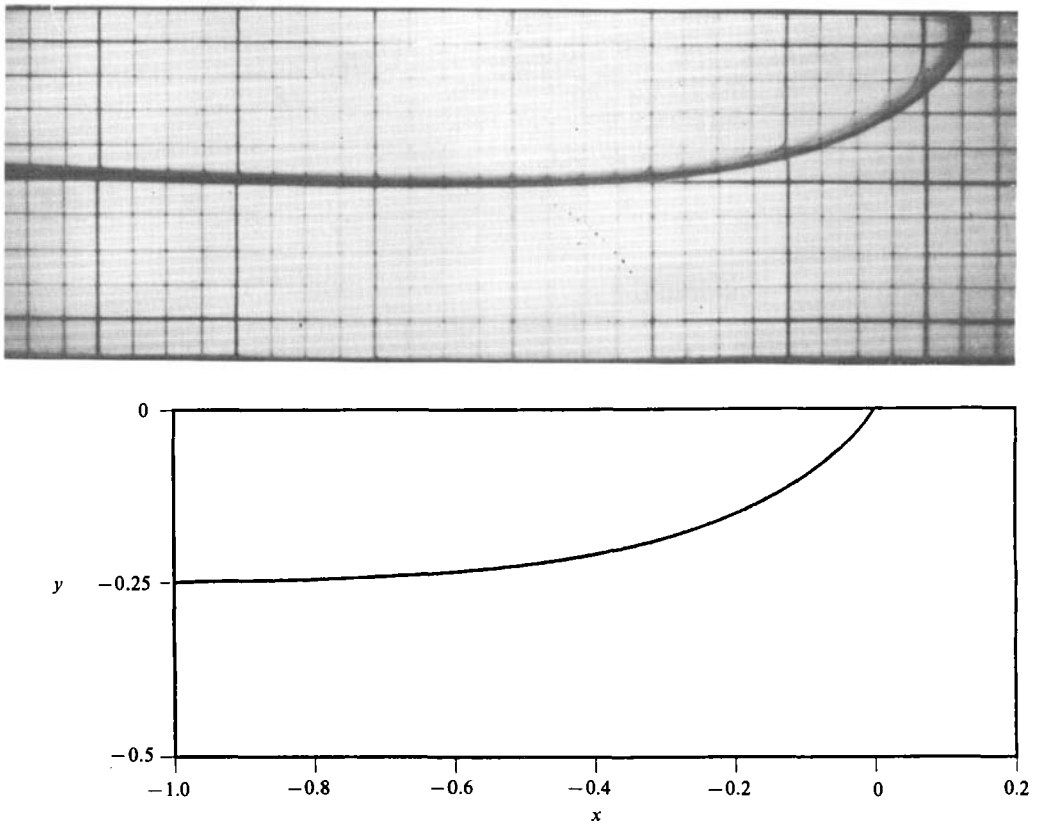

FIGURE 17. Comparison between experimental and numerical bubbles. Photograph is from Maneri (1970) while the solid line is our predicted bubble shape. Inclination angle $\beta = 90°$.

The authors are indebted to Dr A. E. Dukler for first suggesting this problem to them. We also want to thank Dr J.-M. Vanden-Broeck for early discussions on the solution procedure described in §2 and Dr C. C. Maneri for providing us with the photographs of his two-dimensional bubbles.

REFERENCES

BENJAMIN, T. B. 1968 *J. Fluid Mech.* **31**, 209.

BIRKHOFF, G. & CARTER, D. 1957 *J. Math. and Mech.* **6**, 769.

COLLINS, R. 1965 *J. Fluid Mech.* **22**, 763.

COLLINS, R., MORAES, F. F. DE, DAVIDSON, J. F. & HARRISON, D. 1978 *J. Fluid Mech.* **89**, 497.

COUËT, B., STRUMOLO, G. S. & DUKLER, A. E. 1986 *Phys. Fluids* **29**, 2367.

DAVIES, R. M. & TAYLOR, G. I. 1950 *Proc. R. Soc. Lond.* A **200**, 375.

DUMITRESCU, D. T. 1943 *Z. angew. Math. Mech.* **23**, 139.

GARABEDIAN, P. R. 1957 *Proc. R. Soc. Lond.* A **241**, 423.

GRACE, J. R. & HARRISON, D. 1967 *Chem. Engng Sci.* **22**, 1337.

MANERI, C. C. 1970 The motion of plane bubbles in inclined ducts. Ph.D. dissertation, Polytechnic Institute of Brooklyn, New York.

MANERI, C. C. & ZUBER, N. 1974 *Intl J. Multiphase Flow* **1**, 623.

VANDEN-BROECK, J.-M. 1984*a* *Phys. Fluids* **27**, 1090.

VANDEN-BROECK, J.-M. 1984*b* *Phys. Fluids* **27**, 2604.

ZUKOSKI, E. E. 1966 *J. Fluid Mech.* **25**, 821.